ceptibility of $Sr_3CuPt_{0.5}Ir_{0.5}O_6$ follows the predicted behavior of a random quantum spin chain (Figs. 3 and 4). At high temperatures, the susceptibility has a linear χ versus $1/T$ dependence and is Curie-like. In this regime, where there is no ordering among unpaired electrons, the spins act independently. A fit of the high-temperature data gave a Weiss constant of $\theta = -12.7$ K and a spin-only moment of $\mu = 2.11$ Bohr magnetons. This moment is in excellent agreement with that expected for a sample containing, on average, one $S = ½$ Cu ion and one-half $S = ½$ Ir ion, which should yield an effective moment of $\mu = 2.12$. At lower temperatures, there is a transition to a regime where spin-spin interactions become important, as indicated by the broad curve in the inverse susceptibility. This transition marks the alignment of spins to form islands of effective spins, as discussed above. Comparison of Figs. 3 and 4 shows that theory and experiment are in good agreement.

REFERENCES AND NOTES

1. F. D. M. Haldane, *Phys. Lett. A* **93**, 463 (1983); *Phys. Rev. Lett.* **50**, 1153 (1983).
2. M. Hase, I. Terasaki, K. Uchinokura, *Phys. Rev. Lett.* **70**, 3651 (1993); Q. J. Harris *et al.*, *Phys. Rev. B* **50**, 12606 (1994).
3. I. S. Jacobs *et al.*, *Phys. Rev. B* **14**, 3036 (1976).
4. R. J. Birgeneau and G. Shirane, *Phys. Today* **31** (no. 12), 32 (1978).
5. L. N. Bulaevskii, A. V. Zvarykina, Y. S. Karimov, R. B. Lyubovskii, I. F. Shchegolev, *Sov. Phys. JETP* **35**, 384 (1972).
6. M. E. Fisher, *Am. J. Phys.* **32**, 343 (1964).
7. D. S. Fisher, *Phys. Rev. B* **50**, 3788 (1994).
8. C. Dasgupta and S. K. Ma, *ibid.* **22**, 1305 (1980).
9. E. Westerberg, A. Furusaki, M. Sigrist, P. A. Lee, *Phys. Rev. Lett.*, **75**, 4302 (1995).
10. A. Furusaki, M. Sigrist, P. A. Lee, K. Tanaka, N. Nagaosa, *ibid.* **73**, 2622 (1994).
11. T. N. Nguyen, D. M. Giaquinta, H.-C. zur Loye, *Chem. Mater.* **6**, 1642 (1994).
12. T. N. Nguyen and H.-C. zur Loye, *J. Solid State Chem.* **117**, 300 (1995).
13. A. P. Wilkinson, A. K. Cheetham, W. Kunnman, A. Kvick, *Eur. J. Solid State Inorg. Chem.* **28**, 453 (1991).
14. M. Neubacher and H. Müller-Buschbaum, *Z. Anorg. Allg. Chem.* **607**, 124 (1992).
15. Polycrystalline samples of Sr_3CuPtO_6, Sr_3CuIrO_6, and $Sr_3CuPt_{1-x}Ir_xO_6$ ($0 < x < 1$) were prepared through solid state reactions. Stoichiometric amounts of $SrCO_3$ (Cerac, 99.5%), Ir metal (Aesar or Engelhard, 99.9%), Pt metal (Aesar, 99.99%), and CuO (Cerac, 99.999%) were intimately mixed with an agate mortar and pestle under acetone and pressed into pellets. The pellets were placed on platinum foil in alumina boats during heating to prevent aluminum contamination. Heating the samples at 1150°C for 2 weeks with intermittent grindings yielded single-phase materials.
16. Powder samples were structurally characterized with a Rigaku RU300 x-ray diffractometer using Cu K_α radiation (wavelength, 1.5405 Å). The oxygen content of the samples was determined by thermogravimetric analysis (TGA) with a Cahn TG121 system. Samples weighing ~50 to ~100 mg were heated to 900°C in 5% H_2:95% N_2. The initial oxygen content was back-calculated from the measured weight loss. Heating oxygen-deficient samples in pure oxygen to 550° to 700°C resulted in a weight gain associated with the complete oxidation of the compounds.
17. Magnetic measurements were obtained with a Quantum Design MPMS superconducting quantum interference device (SQUID) magnetometer at temperatures from 2 to 300 K. All samples were fully oxidized by annealing in O_2 at 550° to 750°C before use in any magnetic measurements. For data collection, all samples were cooled in zero field to 5 K. When the sample temperature reached 5 K, the magnetic field was turned on and data were collected. All data were corrected for the diamagnetic contribution of the calibrated Kel-F sample container.
18. J. C. Bonner and M. E. Fisher, *Phys. Rev.* **135**, 640 (1964).
19. Strictly speaking, in this compound the ferromagnetic bonds always occur in pairs rather than following a random distribution. However, the physical properties of the two models are expected to be similar.

20. Supported in part by NSF Materials Research Science and Engineering Center award DMR 94-00334 and by the MIT Science Partnership Fund.

28 July 1995; accepted 17 November 1995

Th-Pb and U-Pb Dating of Ore-Stage Calcite and Paleozoic Fluid Flow

Joyce C. Brannon,* Susan C. Cole, Frank A. Podosek,
Virginia M. Ragan, Raymond M. Coveney Jr.,
Malcolm W. Wallace, Alison J. Bradley†

Thorium-232–lead-208 and uranium-238–lead-206 radiometric ages for ore-stage calcite show that Mississippi Valley–type (MVT) ore deposits can form in distinct tectonic settings. An age of 251 ± 11 million years for the Jumbo Mine in Kansas, United States, is in agreement with other ages for MVT deposits in the midcontinent of North America. The similarity of ages of these deposits supports the concept that they formed in response to fluid flow during the late Paleozoic Alleghenian-Ouachita orogeny. An age of 351 ± 15 million years for Twelve Mile Bore and Bloodwood-Kapok deposits in Australia indicates that these MVT ores were deposited in a rifting environment.

Analyses of minerals precipitated from or reacted with fluids provide a key means to determine the composition of the parental fluid and the timing of its flow. The minerals that most commonly precipitate in postdepositional sedimentary rocks are carbonates, sulfides, sulfates, silicates, and fluorite. These are also the major components of MVT ore deposits, which are economically important base-metal deposits generally believed to form from warm basinal brines that are not directly associated with igneous activity (*1*).

Radiometric dating of MVT minerals has been difficult because of low abundances of the natural radioactive isotopes useful for isotopic geochronology. Recently, sphalerite and fluorite in MVT ore deposits have been dated successfully by the Rb-Sr and Sm-Nd techniques, respectively (*2–7*). ^{238}U-^{206}Pb has been used to date late-stage gangue calcite (*8*) and early diagenetic calcite (*9*). Here we report ^{238}U-^{206}Pb and ^{232}Th-^{208}Pb data that yield direct ages for ore-stage calcite. The ability to date an additional ore-stage mineral (that is, calcite) provides the means to date many diverse deposits and is especially important for the chronology of MVT ore deposition for which Sangster has noted, "Evaluation of current and future genetic models for MVT deposits depends first and foremost on reliable determinations of the absolute age of ore emplacement" (*10*).

Ore-stage calcite is generally less common

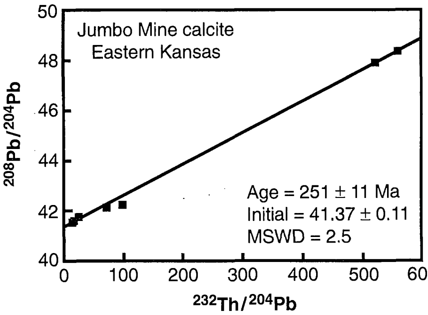

Fig. 1. Th-Pb isochron for ore-stage calcites from the Jumbo Mine, eastern Kansas. Data are from Table 1. Isochron fits were calculated by the York-fit model 1 algorithm of Ludwig (*24*). Ages were calculated for a radioactive decay constant (λ) = 4.9475×10^{-11} year^{-1}. The fit excludes sample JB-8B because the Th value was calculated from a small peak with a rapidly changing background. If JB-8B is included in the regression, the age is 250 ± 22 Ma, and the initial $^{208}Pb/^{206}Pb$ ratio is 41.31 ± 0.19 with a mean standard weighted deviation (MSWD) of 11.

J. C. Brannon, S. C. Cole, F. A. Podosek, Department of Earth and Planetary Sciences and McDonnell Center for the Space Sciences, Washington University, St. Louis, MO 63130-4889, USA.

V. M. Ragan and R. M. Coveney Jr., Department of Geosciences, University of Missouri, Kansas City, MO 64110-2499, USA.

M. W. Wallace and A. J. Bradley, School of Earth Sciences, University of Melbourne, Parkville, Victoria 3052, Australia.

---

*To whom correspondence should be addressed.

†Present address: Hamersley Iron, Post Office Box 181, Tom Price, Western Australia 6751, Australia.

than is ubiquitous late-stage calcite in MVT ore deposits. It is distinguishable from late-stage calcite because the temperatures and salinities of its fluid inclusions are similar to those found in sphalerite from the same deposits, and textures indicate formation contemporaneous with ore deposition. In contrast, late-stage calcite precipitates after ore deposition and contains fluid inclusions that are typically cooler and less saline than those found in sphalerite from the same deposit.

The Jumbo Mine, hosted by Middle Pennsylvanian rocks of eastern Kansas, is a distal Zn-Pb occurrence of the Tri-State MVT district of Missouri, Kansas, and Oklahoma, which produced more than 3.7 million tons of Zn-Pb concentrates from 1848 to 1967 (*11*). Similar Pb isotopic compositions from both the Tri-State district and the Jumbo Mine indicate a common source for the mineralizing brines (*12*). Results for U, Th, and Pb in Jumbo Mine ore-stage calcites (Table 1 and Fig. 1) yield an isochron age of 251 ± 11 million years ago (Ma), and an initial $^{208}Pb/^{204}Pb$ ratio (41.37 ± 0.11) consistent with the range for $^{208}Pb/^{204}Pb$ ratios in galena from the Tri-State district ($^{208}Pb/^{204}Pb$ = 41.07 to 41.38) (*13*). The ore-stage calcite as well as sphalerite, barite, and dolomite at Jumbo Mine contain petroleum-bearing fluid inclusions in addition to the ubiquitous brine inclusions. Hence, the ^{232}Th-^{208}Pb age of the calcite dates the mineralization at the Jumbo Mine and also establishes a time for the migration of petroleum in eastern Kansas.

The ^{232}Th-^{208}Pb age for ore deposition in the Tri-State region, along with a ^{87}Rb-^{86}Sr age for sphalerite from the Upper Mississippi Valley Zn-Pb district (270 ± 4 Ma) (*3*) and a ^{147}Sm-^{143}Nd age for fluorite from the Illinois-Kentucky fluorspar (IKF) district (272 ± 17 Ma) (*6*), all indicate formation of MVT ore deposits during the late Paleozoic Alleghenian-Ouachita orogeny (325 to 250 Ma). Paleomagnetic ages for MVT districts in the midcontinent of North America (Northern Arkansas, Central Missouri, Southeast Missouri, and Central Tennessee) are also consistent with the time of this orogeny, the IKF district being the only exception (*14*). The broad agreement of both radiometric and paleomagnetic ages for MVT deposits over hundreds of kilometers in the midcontinent of North America is consistent with the idea that the orogeny caused brine and oil migration and MVT formation (*15*).

Table 1. U, Th, and Pb data for ore-stage calcite from the Jumbo Mine, eastern Kansas (*25*). Concentrations by isotope dilution are in parts per 10^9. Two standard deviation errors in parenthesis are for last digits listed. Pb isotopic analyses are by the silica gel method with data adjusted for 0.75 [per mil per atomic mass unit (amu)] fractionation.

Sample	[U]	[Th]	[Pb]	$^{232}Th/^{204}Pb$	$^{206}Pb/^{204}Pb$	$^{207}Pb/^{204}Pb$	$^{208}Pb/^{204}Pb$
JB-8A	0.88(1)	216(3)	218.3(7)	71.4(1.2)	22.03(2)	15.92(3)	42.12(11)
JB-8B	2.42(2)	226(3)	165.5(5)	98.0(1.3)	21.58(3)	15.98(3)	42.23(10)
JB-10Z1A	1.52(1)	165(3)	839(6)	14.2(2)	22.33(3)	15.95(3)	41.53(8)
JB-10Z1B	1.30(3)	130(3)	392(2)	24.1(6)	22.37(3)	15.98(3)	41.75(9)
JB-10Z2	1.50(2)	292(4)	1344(5)	16.5(2)	22.40(2)	15.97(3)	41.59(9)
JB-11B	2.18(2)	293(4)	41.0(1)	560(8)	22.27(8)	16.02(6)	48.36(21)
JB-11C	2.34(4)	310(4)	46.3(1)	522(7)	22.31(4)	15.99(3)	47.90(12)

Table 2. U and Pb data for ore-stage calcite and galena from Twelve Mile Bore and Bloodwood-Kapok MVT deposits, Western Australia (*25*). Concentrations by isotope dilution are in parts per 10^9. Two-standard-deviation errors in parenthesis are for the last digits listed. Pb isotopic analyses are by the silica gel method with data adjusted for 0.75 per mil/amu fractionation.

Sample	[U]	[Pb]	$^{238}U/^{204}Pb$	$^{206}Pb/^{204}Pb$	$^{207}Pb/^{204}Pb$	$^{208}Pb/^{204}Pb$
			Calcite			
PCD064-183.15A	111.6(6)	90.1(3)	88.1(6)	23.93(8)	16.00(6)	40.75(17)
PCD064-183.15A2	124(2)	51.0(2)	193(4)	30.47(13)	16.46(8)	43.29(22)
PCD064-183.15A3	125.8(6)	134.0(6)	65.4(4)	22.95(3)	16.03(3)	40.77(9)
PCD064-183.15B	124.5(7)	574(3)	14.2(1)	19.91(5)	15.75(5)	39.39(15)
PCD180-170.40A	166(9)	1202(7)	9.2(5)	19.70(4)	15.78(4)	39.41(13)
PCD180-170.40B	118.4(9)	577(2)	13.5(1)	19.82(5)	15.79(5)	39.39(14)
PCD122-107.4A	37.1(5)	141.2(5)	17.5(2)	20.13(3)	15.89(3)	39.93(9)
PCD122-107.4B	42(1)	395(2)	7.0(3)	19.63(2)	15.88(3)	39.65(8)
PCD122-107.20A	165.5(9)	620(3)	17.7(1)	20.24(2)	15.91(2)	39.63(8)
PCD122-107.0A	72.9(6)	809(6)	5.88(7)	19.61(2)	15.86(3)	39.59(8)
ID553-695.7A	80.9(4)	190.9(6)	28.6(2)	20.74(6)	15.84(5)	39.29(15)
ID553-695.7A2	50.8(3)	165.6(6)	20.3(2)	20.35(4)	15.84(4)	39.32(13)
ID553-695.7A3	71.3(6)	170.6(6)	27.8(3)	20.76(4)	15.89(4)	39.41(13)
			Galena			
PCD 122-107.4C4				19.33(2)	15.85(2)	39.57(8)
PCD 180-170.40E				19.32(2)	15.84(2)	39.52(8)

MVT mineralization is also widespread in the Upper Devonian reefs of the Lennard Shelf in Western Australia. The age of mineralization across the Lennard Shelf has been constrained by correlation of the diagenetic, thermal, and burial histories of the Devonian carbonates with cathodoluminescent calcite cement stratigraphy to be 350 ± 15 Ma, that is, when the carbonates were subjected to burial diagenesis (*16*). Tompkins *et al.* (*17*) disputed this conclusion and suggested that mineralization had occurred not only during subsidence but also during subsequent uplift, and they also suggested that two of the larger deposits (Blendevale and Cadjebut) were geologically younger (325 ± 25 Ma). More recently, however, Rb-Sr dating of sphalerite from the Blendevale deposit has indicated an age of 357 ± 3 Ma, supporting an earlier mineralization event (*7*).

We obtained a ^{238}U-^{206}Pb age for ore-stage calcite cements from Bloodwood-Kapok (considered the same system as Cadjebut) and Twelve Mile Bore deposits of 351 ± 15 Ma (Table 2 and Fig. 2). The initial $^{206}Pb/^{204}Pb$ ratio (19.23 ± 0.06) marginally overlaps the range found for galena at the Twelve Mile Bore and Cadjebut deposits (19.30 to 19.37) (*17*). The relatively homogeneous Pb isotopic composition for three deposits over a distance of 15 km is consistent with a single source for Pb for the three deposits that are all adjacent to the Cadjebut Fault.

The Fitzroy Trough, which flanks the Lennard Shelf, underwent major extension, rifting, and subsidence during the Middle to Late Devonian (Pillara Extension) (*18, 19*). Post-rift sagging and intermittent rifting continued during the Early Carboniferous. Later during the Carboniferous, compression produced regional uplift and erosion (Meda Transpression) (*18*). Thus, the Late Devonian–Early Carboniferous radiometric age for sphalerite and ore-stage calcite cements indicates that MVT mineralization on the Lennard Shelf

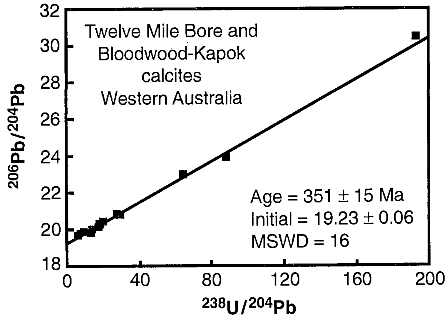

Fig. 2. U-Pb isochron for ore-stage calcite from Twelve Mile Bore and Bloodwood-Kapok deposits in Western Australia. Data are from Table 2. Isochron fits were calculated by the York-fit model 1 algorithm of Ludwig (*24*). Ages were calculated for λ = 1.55125 × 10^{-10} year^{-1}.

occurred in an extensional rift setting. This setting is not consistent with models for the formation of MVT mineralization in which gravity-driven fluid flow is initiated by compressional tectonism (*15*, *20*). Compaction-driven fluid flow due to rapid sedimentation during subsidence (*21*) may be the mechanism that transported base metals out of the Fitzroy Trough to the Lennard Shelf. This mineralization age is not consistent with the hydrocarbon-driven fluid flow model in which MVT mineralization of the Lennard Shelf was linked to a mid-Carboniferous sea level drop and consequent rapid generation of hydrocarbons within the Fitzroy Trough (*22*).

Radiometric ages for ore-stage minerals in MVT deposits have been obtained only in the last 5 years. In providing a test for the temporal relation between hypothesized cause and effect, these ages, along with recent paleomagnetic ages, have been a major force in driving the evolution of genetic models; for example, from a model in which one orogeny formed all MVT deposits in the United States (*2*), to a model in which MVT deposits formed in various orogenies at different times in Earth's history (with the implication that MVT deposits can only be formed by means of an orogeny) (*3*–*6*, *14*), to a model that infers they can also form in a rifting environment (*7*, *16*, *23*).

The ^{232}Th-^{208}Pb and ^{238}U-^{206}Pb dating methods may also have considerable value for determining the absolute ages of calcite found in other geologic settings, including other kinds of ore deposits, salt domes, fault zones, speleothems, and petroleum reservoir rocks. The analytical approach is applicable to calcite of any geologic age and so extends calcite geochronology beyond the U-Th disequilibrium method.

REFERENCES AND NOTES

1. D. A. Sverjensky, *Ann. Rev. Earth Planet. Sci.* **14**, 177 (1986).
2. S. Nakai, A. N. Halliday, S. E. Kesler, H. D. Jones, *Nature* **346**, 354 (1990).
3. J. C. Brannon, F. A. Podosek, R. K. McLimans, *ibid.* **356**, 509 (1992).
4. S. Nakai *et al.*, *Geochim. Cosmochim. Acta* **57**, 417 (1993).
5. J. N. Christensen, A. N. Halliday, S. E. Kesler, D. F. Sangster, *Geol. Soc. Am. Abstr. Prog.* **25**, 471 (1993).
6. J. T. Chesley, A. N. Halliday, T. K. Kyser, P. G. Spry, *Econ. Geol.* **89**, 1192 (1993).
7. J. N. Christensen, A. N. Halliday, J. R. Vearncombe, S. E. Kesler, *ibid.* **90**, 877 (1995).
8. J. C. Brannon, F. A. Podosek, R. K. McLimans, in *Proceedings of the Geology and Geochemistry of MVT Ore Deposits*, Geological Society of America, Rolla, MO, 29 and 30 March 1993, K. Shelton and R. Hagni, Eds. (Univ. of Missouri–Rolla Press, Rolla, MO, 1993), pp. 95–103.
9. P. E. Smith, R. M. Farquhar, R. G. Hancock, *Earth Planet. Sci. Lett.* **105**, 474 (1991).
10. D. F. Sangster, in *Geology and Genesis of Mineral Deposits in Ireland*, C. J. Andrew, R. W. A. Crowe, S. Finlay, W. M. Pennell, J. F. Pyne, Eds. (Irish Association for Economic Geology, Dublin, Ireland, 1986), pp. 625–633.
11. R. D. Hagni and O. R. Grawe, *Econ. Geol.* **59**, 449 (1964); S. R. Blasch and R. M. Coveney Jr., *Geochim. Cosmochim. Acta* **52**, 1007 (1988); D. C. Brockie, E. H. Hare, J. R. Dingess, in *Ore Deposits of the United States 1933–1967*, J. D. Ridge, Ed. (American Institute of Mining, Metallurgical, and Petroleum Engineers, New York, 1968), vol. 1, pp. 400–430; V. M. Ragan, *Econ. Geol.* **89**, 1411 (1994).
12. E. E. Angino, E. D. Goebel, T. C. Waugh, in *Proceedings of the Third International Geochemical Exploration Symposium*, Toronto, Canada, 16 to 18 April 1970, R. W. Boyle and J. I. McGerrigle, Eds. (Canadian Institute of Mining and Metallurgy, Toronto, 1971), pp. 453–456.
13. M. B. Goldhaber *et al.*, *Econ. Geol.*, in press.
14. M. J. Wisniowiecki, R. Van der Voo, C. McCabe, W. C. Kelly, *J. Geophys. Res.* **88**, 6540 (1983); H. Pan, D. T. A. Symons, D. F. Sangster, *Can. J. Earth Sci.* **27**, 923 (1990); D. T. A. Symons and D. F. Sangster, *Econ. Geol.* **86**, 1 (1991); M. T. Lewchuk and D. T. A. Symons, *Geology* **23**, 233 (1995); D. T. A. Symons, *Econ. Geol.* **89**, 438 (1994).
15. D. L. Leach and E. L. Rowan, *Geology* **14**, 931 (1986); J. Oliver, *ibid.*, p. 99; C. M. Bethke and S. A. Marshak, *Ann. Rev. Earth Planet. Sci.* **18**, 287 (1990); J. Oliver, *Earth Sci. Rev.* **32**, 77 (1992); G. Garven, *Ann. Rev. Earth Planet. Sci.* **23**, 89 (1995).
16. A. McManus and M. W. Wallace, *Econ. Geol.* **87**, 189 (1992).
17. L. A. Tompkins, V. A. Pedone, M. T. Roche, D. I. Groves, *ibid* **89**, 450 (1994).
18. J. M. Kennard, M. J. Jackson, K. K. Romine, R. D. Shaw, P. N. Southgate, in *The Sedimentary Basins of Western Australia, Proceedings of the Western Australian Basins Symposium*, Petroleum Exploration Society of Australia, Perth, Western Australia, 14 to 17 August 1994, P. G. Purcell and R. R. Purcell, Eds. (Petroleum Exploration Society of Australia, Perth, Western Australia, 1994), pp. 657–676.
19. J. Begg, *J. Aust. Pet. Explor. Assoc.* **28**, 137 (1987).
20. D. A. Sverjensky and G. Garvin, *Nature* **356**, 481 (1992).
21. L. M. Cathles and A. T. Smith, *Econ. Geol.* **78**, 983 (1983).
22. B. N. Eisenlohr, L. A. Tompkins, L. M. Cathles, M. E. Barley, D. I. Groves, *Geology* **22**, 315 (1994).
23. J. C. Brannon, S. C. Cole, F. A. Podosek, in *Extended Abstracts of the International Field Conference on Carbonate-Hosted Lead-Zinc Deposits*, Society of Economic Geologists, St. Louis, MO, 3 to 6 June 1995 (Society of Economic Geologists, Littleton, CO, 1995), pp. 27–29.
24. K. R. Ludwig, *U.S. Geol. Surv. Open-File Rep. 88-557* (1988).
25. After dissolution, the calcite solutions were spiked with a mixed ^{230}Th, ^{233}U, ^{236}U, ^{205}Pb tracer solution. Anion exchange chromatography was used to separate U, Th, and Pb from the calcite-spike mix solution. Isotopic analyses for samples from the Jumbo Mine were performed on the Washington University VG 354 thermal emission mass spectrometer with a Daly detector in pulse counting mode; those for samples from Western Australia were performed in single collector mode with a Faraday cup for ion detection.
26. We appreciate the assistance and advice given by M. Tatsumoto, W. Premo, and D. A. Papanastassiou. Supported by NSF grant EAR 93 15048 and University of Missouri-Kansas City Women's Council.

23 August 1995; accepted 30 November 1995

Redox Stabilization of the Atmosphere and Oceans by Phosphorus-Limited Marine Productivity

Philippe Van Cappellen* and Ellery D. Ingall

Data from modern and ancient marine sediments demonstrate that burial of the limiting nutrient phosphorus is less efficient when bottom waters are low in oxygen. Mass-balance calculations using a coupled model of the biogeochemical cycles of carbon, phosphorus, oxygen, and iron indicate that the redox dependence of phosphorus burial in the oceans provides a powerful forcing mechanism for balancing production and consumption of atmospheric oxygen over geologic time. The oxygen-phosphorus coupling further guards against runaway ocean anoxia. Phosphorus-mediated redox stabilization of the atmosphere and oceans may have been crucial to the radiation of higher life forms during the Phanerozoic.

The fossil and sedimentary records imply that the oxygen level of the atmosphere has remained within a fairly narrow range during most of the Phanerozoic (*1*, *2*). The presence of higher plants and animals on land, for instance, imposes stringent limits on the atmospheric partial pressure of oxygen (P_{O_2}) at least since the end of the Devonian. In contrast, early attempts at reconstructing past atmospheric oxygen levels that used simple carbon-plus-sulfur isotope mass-balance models revealed imbalances in the rates of production and consumption of atmospheric oxygen, which should have resulted in unacceptably large fluctuations of P_{O_2} over the course of the Phanerozoic (*3*, *4*). In order to avoid unrealistic excursions of P_{O_2}, negative feedbacks have been included in oxygen mass-balance models (*4*, *5*). Mathematically, the feedbacks help reconcile the mass-balance calculations with the geologic evidence, but the true mechanisms that stabilize atmospheric P_{O_2} have been elusive (*6*). Here we show that the marine phosphorus cycle may contain the key oxygen controls, through its involvement in oceanic primary productivity.

The availability of phosphorus limits net primary production of the global ocean on

---

P. Van Cappellen, School of Earth and Atmospheric Sciences, Georgia Institute of Technology, Atlanta, GA 30332-0340, USA.
E. D. Ingall, Marine Science Institute, University of Texas at Austin, Port Aransas, TX 78373-1267, USA.

*To whom correspondence should be addressed.